9-2-2011

A comparative study of enzyme immobilization strategies for multi-walled carbon nanotube glucose biosensors

Jin Shi
Birck Nanotechnology Center, Purdue University, shij@purdue.edu

Jonathan C. Claussen
Birck Nanotechnology Center, Purdue University, jclausse@purdue.edu

Eric S. McLamore
University of Florida

Aeraj ul Haque
Birck Nanotechnology Center, Purdue University

David Jaroch
Birck Nanotechnology Center, Purdue University, djaroch@purdue.edu

See next page for additional authors

Shi, Jin; Claussen, Jonathan C.; McLamore, Eric S.; ul Haque, Aeraj; Jaroch, David; Diggs, Alfred; Calvo-Marzal, Percy; Rickus, Jenna; and Porterfield, D. Marshall, "A comparative study of enzyme immobilization strategies for multi-walled carbon nanotube glucose biosensors" (2011). *Birck and NCN Publications.* Paper 955.
http://dx.doi.org/10.1088/0957-4484/22/35/355502

Authors
Jin Shi, Jonathan C. Claussen, Eric S. McLamore, Aeraj ul Haque, David Jaroch, Alfred Diggs, Percy Calvo-Marzal, Jenna Rickus, and D. Marshall Porterfield

A comparative study of enzyme immobilization strategies for multi-walled carbon nanotube glucose biosensors

2011 Nanotechnology 22 355502

(http://iopscience.iop.org/0957-4484/22/35/355502)

Nanotechnology **22** (2011) 355502 (10pp) doi:10.1088/0957-4484/22/35/355502

A comparative study of enzyme immobilization strategies for multi-walled carbon nanotube glucose biosensors

Jin Shi[1,2], Jonathan C Claussen[2,3], Eric S McLamore[4], Aeraj ul Haque[2,3], David Jaroch[1,2], Alfred R Diggs[2,3], Percy Calvo-Marzal[5], Jenna L Rickus[1,2,3] and D Marshall Porterfield[1,2,3,6]

[1] Weldon School of Biomedical Engineering, Purdue University, USA
[2] Physiological Sensing Facility, Bindley Bioscience Center and Birck Nanotechnology Center, Purdue University, USA
[3] Department of Agricultural and Biological Engineering, Purdue University, USA
[4] Department of Agricultural and Biological Engineering, University of Florida, USA
[5] Department of Chemistry, Purdue University, USA
[6] Department of Horticulture and Landscape Architecture, Purdue University, USA

E-mail: porterf@purdue.edu

Received 25 April 2011, in final form 21 July 2011
Published 9 August 2011
Online at stacks.iop.org/Nano/22/355502

Abstract

This work addresses the comparison of different strategies for improving biosensor performance using nanomaterials. Glucose biosensors based on commonly applied enzyme immobilization approaches, including sol–gel encapsulation approaches and glutaraldehyde cross-linking strategies, were studied in the presence and absence of multi-walled carbon nanotubes (MWNTs). Although direct comparison of design parameters such as linear range and sensitivity is intuitive, this comparison alone is not an accurate indicator of biosensor efficacy, due to the wide range of electrodes and nanomaterials available for use in current biosensor designs. We proposed a comparative protocol which considers both the active area available for transduction following nanomaterial deposition and the sensitivity. Based on the protocol, when no nanomaterials were involved, TEOS/GOx biosensors exhibited the highest efficacy, followed by BSA/GA/GOx and TMOS/GOx biosensors. A novel biosensor containing carboxylated MWNTs modified with glucose oxidase and an overlying TMOS layer demonstrated optimum efficacy in terms of enhanced current density (18.3 ± 0.5 μA mM^{-1} cm^{-2}), linear range (0.0037–12 mM), detection limit (3.7 μM), coefficient of variation (2%), response time (less than 8 s), and stability/selectivity/reproducibility. H_2O_2 response tests demonstrated that the most possible reason for the performance enhancement was an increased enzyme loading. This design is an excellent platform for versatile biosensing applications.

1. Introduction

Glucose plays a central role in metabolism, and glycolytic transport is commonly studied in cancer research (e.g., the Warburg effect), diabetes, and other cell/tissue culture applications [5]. Electrochemical glucose biosensors are a vital tool for measuring glucose for a wide range of applications, including point of care diagnostics and preventative disease research [7, 23]. Most biosensors are based on enzymatic recognition of glucose by glucose oxidase (GOx), where oxidation to gluconic acid produces H_2O_2, which is detected using oxidative amperometry at a potential of +0.5–0.8 V [43, 17, 28, 37]. As a result of the ongoing research focused on the development of glucose biosensors [13, 42, 15, 43, 28, 37, 9, 10], GOx has emerged as the *de facto* standard enzyme for exploring

oxidative enzyme immobilization strategies. While enzyme immobilization protocols and transduction schemes are not completely interchangeable, immobilization approaches successfully demonstrated with glucose biosensors can potentially be applied to other biosensors for sensing important physiological compounds.

Enzymes such as GOx are typically immobilized on electrodes (e.g. platinum discs) via chemical linkage [27, 9] or physical entrapment within a polymeric matrix [28, 37, 33, 6]. Glutaraldehyde (GA) is a commonly used amine cross-linking agent which links enzymes via Schiff bases [24]. Bovine serum albumin (BSA) is often used with GA to solubilize/stabilize enzymes, because GA may potentially lead to enzyme deformation and non-specific binding [16, 31]. Covalent immobilization via BSA/GA linkages significantly improves the consistency of biosensors [34, 35, 27].

Silicate sol–gels formed by ethyl esters of orthosilicic acid, including tetraethyl orthosilicate (TEOS) [33] and tetramethyl orthosilicate (TMOS) [6], are commonly used for immobilizing enzymes via physical adsorption, because the hydrolysis/condensation reaction of sol–gels generates a three-dimensional polymer matrix of silica. Molecules immobilized in TEOS/TMOS polymers are not chemically modified; thus the porous structure of the matrix entraps enzymes while facilitating diffusion of analytes such as glucose and H_2O_2 [32].

Sensor performance can be enhanced by incorporating various nanomaterials [13, 28, 37, 43, 15, 9]. Carbon nanotube (CNT) is a nanomaterial which enhances biosensor performance by facilitating electron transfer [44, 43, 15]. The widespread use of CNTs in a variety of applications [12, 41] has improved our understanding of the mechanisms involved in this facilitated electron transfer, significantly improving the efficiency of enzymatic biosensors [13, 10, 48, 9, 45, 44, 14, 27, 28, 36, 26]. When used in biosensors, CNTs can directly immobilize enzymes by forming highly porous and inert carbon matrices [45], which provide enzyme immobilization via physical entrapment, and/or peptide bond formation between enzymatic amine groups and carboxyl groups of functionalized CNTs [13]. CNT matrices often include Nafion for charge exclusion (e.g., ascorbate and acetaminophen) [29] and increased matrix chemical/mechanical stability [20]. In addition, Nafion is commonly used because it does not significantly swell following immersion in aqueous solutions, and is highly permeable to water [20, 4, 44, 39, 21]. Thus, Nafion is often used in biosensors for incorporating relatively insoluble CNTs.

Due to the multitude of possible combinations for utilizing these nanomaterials/polymers in biosensors, a comprehensive comparison of rational fabrication schemes is needed for developing reproducible and reliable enzymatic biosensors. Sensitivity is the gold standard for comparing various biosensor designs, although reported sensitivities for GOx biosensors vary greatly, e.g., from 0.33 μA mM^{-1} in a study by Tsai *et al* [39] to 2.11 μA mM^{-1} in a study by Hrapovic *et al* [17]. Another parameter that is commonly used is electrode surface area, which also varies greatly, e.g., from 12×10^{-2} cm^2 in Wang *et al* [45] to 3.14×10^{-2} cm^2 in Zhang *et al* [46]. The synergy between active transduction area (i.e., surface area) and properly immobilized enzymes (available binding pockets) regulates overall biosensor efficacy. Although sensitivity is commonly reported, there is currently not a consistent protocol for comparing biosensor performance based on both sensitivity and surface area.

This study compares the performance of commonly used biosensor fabrication schemes utilizing MWNTs, silica sol–gels (TEOS and TMOS), and BSA/GA enzymatic linking. Direct comparison of biosensor efficiency based on a comprehensive protocol which considers sensitivity and effective surface area will lead to improved biosensor design by the inclusion of nanomaterials. Using this approach, highly efficient GOx biosensor design schemes can be extrapolated to other enzymatic biosensors for the detection of analytes such as adenosine triphosphate (ATP) [22], ethanol [1, 20] and glutamate [4, 11, 27].

2. Materials and methods

2.1. Chemicals and reagents

Deionized water of resistivity 18.2 MΩ cm (Milli-Q) was used to prepare solutions. Glucose oxidase (E.C.1.1.3.4, 2000–10 000 units g^{-1}, from *Aspergillus niger*), potassium chloride (KCl, 99%), potassium ferricyanide ($K_3Fe(CN)_6$), Nafion (5% wt/wt), tetraethyl orthosilicate (⩾99%), tetramethyl orthosilicate (⩾99%), hydrochloric acid (HCl), hydrogen peroxide (H_2O_2), bovine serum albumin and glutaraldehyde (Grade II, 25% aqueous solution) were purchased from Sigma-Aldrich (St Louis, MO). D-glucose and sodium chloride (NaCl) were purchased from Mallinckrodt Baker, Inc (Phillipsburg, NJ). Sodium phosphate ($Na_2HPO_4\cdot7H_2O$) and potassium phosphate (KH_2PO_4, monobasic) were purchased from Fisher Chemicals (Pittsburg, PA). PBS solution (0.01 M) was prepared by dissolving 8 g NaCl, 1.15 g Na_2HPO_4, 0.2 g KCl and 0.2 g KH_2PO_4 in 1 l deionized water. MWNTs (–COOH functionalized MWNTs, 95 wt%, 8–15 nm OD) were purchased from cheaptubes.com.

2.2. Fabrication of biosensors

A Pt electrode was used as the transduction element for the biosensor, which consisted of a polished Pt plate (3 mm diameter) soldered to a copper wire with a glass encapsulation. Before modification, the Pt electrode was polished with 1, 0.3 and 0.05 μm alumina slurries for 1 min each, and then ultrasonicated in ethanol and deionized water for 1 min each.

For the TEOS/GOx (or TMOS/GOx) biosensors, 1 ml of TEOS (or 1 ml of TMOS) was mixed with 200 μl-DI (or 300 μl for TMOS) and 25 μl (or 27 μl for TMOS) of 0.4 N HCl to maintain the same molar ratio (1:2.48) between sol–gel and H_2O. This mixture was ultrasonicated for 15 min and aged at 4 °C for 72 h before use. The pre-treated solution (60 μl) was then mixed with 60 μl of 46 mg-GOx/ml-PBS. Polished Pt electrodes were then dipped into the mixture for 12 h and air dried for 30 min before use.

For the BSA/GA/GOx biosensors, a solution was prepared by mixing 40 μl of 25 mg ml^{-1} BSA, 20 μl of 2.5% glutaraldehyde (GA), and 60 μl of 46 mg-GOx/ml-PBS. Polished electrodes were dipped into the mixture for 12 h, and then taken out and air dried for 30 min before use.

For the bionanocomposite CNT–TMOS (or TEOS) biosensors, MWNTs (2 mg) were mixed with 1 ml Nafion, and ultrasonicated for 30 min. The MWNT/Nafion mixture (2 μl) was deposited on the surface of a Pt electrode and air dried for 10 min. The electrode was then dipped in 46 mg-GOx/ml-PBS solution for 1 h, and the electrode was then modified using a TMOS (or TEOS) solution as described above. When not in use, the biosensors were stored in 46 mg-GOx/ml-PBS solution at 4 °C.

For the CNT–GA biosensors, MWNTs (2 mg) were mixed with 1 ml Nafion, and ultrasonicated for 30 min. The MWNT/Nafion mixture (2 μl) was deposited on the surface of a Pt electrode and air dried for 10 min. A solution was prepared by mixing 40 μl of 25 mg ml^{-1} BSA, 20 μl of 2.5% glutaraldehyde (GA), and 60 μl of 46 mg-GOx/ml-PBS. Polished electrodes were dipped into the mixture for 12 h, and then taken out and air dried for 30 min before use.

For Pt/MWNT/Nafion electrode, MWNT (2 mg) were mixed with 1 ml Nafion, and ultrasonicated for 30 min. The MWNT/Nafion mixture (2 μl) was deposited on the surface of a Pt electrode and air dried for 10 min.

2.3. Calibration and selectivity

DC potential amperometry and cyclic voltammetry (CV) were performed on a three electrode electrochemical (C-3) cell stand (BASi, West Lafayette, IN). Ag/AgCl reference electrode and auxiliary electrodes were purchased from BASi. DC potential amperometry was carried out with a working potential of +500 mV versus the Ag/AgCl reference electrode with a sampling rate of 1 kHz. CV was carried out with 10 s quiet time at different scan rates using methods common to the literature [40].

Amperometric sensitivity toward glucose was determined by measuring current at a constant working potential (+500 mV) while sequentially adding glucose. Complete mixing of the solution was ensured through constant stirring at 400 rpm with a magnetic stirrer. The measured current signal was allowed to reach steady state following each glucose addition, and average current represents the arithmetic mean of steady state observed current. For all experiments, steady state was defined as less than a 3% change in measured current for a 60 s time period. All error bars represent the standard error of the mean (SEM), and n values are reported where applicable. Average current versus glucose concentration was used to characterize sensitivity, and the slope of each linear calibration curve used to estimate sensitivity (nA mM^{-1}). For each enzyme immobilization approach, three replicate biosensors were fabricated on the same electrode after it was polished, and average sensitivity was reported. The difference in performance was reported as the standard error of the mean in sensitivity.

Selectivity over ascorbic acid and acetaminophen was tested by calibrating via DC potential amperometry in the presence of 6 μM ascorbic acid (physiological concentration) and 10 μM acetaminophen (therapeutic concentration). Ascorbic acid and acetaminophen were added to PBS solutions containing 1 mM glucose.

2.4. Surface area and current density determination

Effective surface area was determined by CV in 4 mM $Fe(CN)_6^{3-}$/1 M KNO_3 solution in the potential range of 0 to +650 mV. The reduction peak current (i_p) was determined by the Randles–Sevcik equation [2]

$$i_p = (2.69 \times 10^5) n^{3/2} D^{1/2} C A v^{1/2} \quad (1)$$

where n is the number of transferred electrons for the redox reaction, D is the diffusion coefficient (6.70×10^{-6} cm^2 s^{-1}), C is the molar concentration of ferricyanide (4 mM), A is the effective surface area (cm^2), and v is the scan rate (V s^{-1}). For CV using $Fe(CN)_6^{3-}$, the value of n is equal to one, due to the following half reaction taking place at the electrode:

$$Fe(CN)_6^{3-} + e^- \rightarrow Fe(CN)_6^{4-}. \quad (2)$$

From equation (1), a well-established linear relationship exists between i_p and $v^{1/2}$. By performing linear regression for i_p versus $v^{1/2}$, the slope k can be obtained, and one may express A as

$$A = k/((2.69 \times 10^5) n^{3/2} D^{1/2} C). \quad (3)$$

A series of scan rates (v = 20, 50, 100, 125, 150 and 200 mV s^{-1}) was used, and the corresponding i_p recorded, where the scan rates were similar to previous studies [40]. To compare the efficiency of various electrode designs based on sensitivity and surface area, the current density was defined as

$$K = i/A \quad (4)$$

where K is the current density (μA mM^{-1} cm^{-2}), i is the amperometric sensitivity (μA mM^{-1}) and A is the effective surface area of the electrode after surface modification. This parameter (K) describes the efficacy of biosensors in terms of sensitivity and surface area, and may be used across a wide range of spatial scales (i.e., macrosensor and/or microsensor applications).

2.5. Imaging

All field emission scanning electron microscopy (FESEM) graphs of the bionanocomposite CNT–TMOS biosensor were obtained from a Hitachi S-4800 microscope with a power setting of 5.0 kV and magnification settings of 3.5k and 25k. The biosensor was prepared on a Pt electrode, and fixed in a vertical position for imaging (no additional preprocessing).

3. Results and discussion

3.1. Comparison of effective surface area

CVs for bare electrodes (specified radius of 1.5 mm) in ferricyanide followed expected trends (appendix figure A.1(a)),

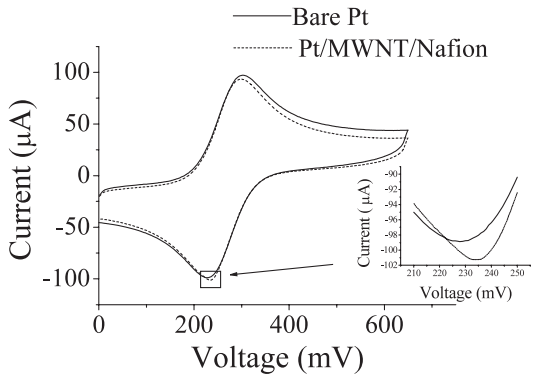

Figure 1. Representative CV for a bare Pt electrode and a Pt/MWNT/Nafion electrode in 4 mM $K_3Fe(CN)_6$/1 M KNO_3 at a scan rate of 200 mV s^{-1}. Inset: exploded view of the reduction peak.

and plots of peak current versus square root of scan rate were linear (appendix figure A.1(b)). Using equation (3), the effective surface area and radius of the bare Pt electrode were 7.20 ± 0.18 mm^2 and 1.51 ± 0.02 mm, respectively, validating the use of the Randles–Sevcik approach for determining electrode effective surface area. CV curves for bare Pt and Pt/MWNT/Nafion electrodes in 4 mM $Fe(CN)_6^{3-}$/1 M KNO_3 at a scan rate of 200 mV s^{-1} are presented in figure 1. As expected, well-defined reduction and oxidation peaks were observed, and the mean value of peak separation for bare Pt (70.3 ± 1.0 mV) was higher than values for Pt/MWNT/Nafion electrodes (62.7 ± 2.8 mV). This was due to changes of the surface micro-structure layer on the metal electrode which likely affected the semi-infinite linear diffusion-controlled redox of $Fe(CN)_6^{3-}$/$Fe(CN)_6^{4-}$, and resulted in a smaller peak separation [14]. As expected, this indicated enhanced electrochemical reversibility for the Pt/MWNT/Nafion electrode over the bare Pt electrode.

Using this technique, the electrode effective surface area was determined for each sensor design following modification using various nanomaterials/polymers/GOx. Immobilization of MWNTs in the Nafion layer increased the effective area (by an average of 11 ± 3%). These results were expected, as CNTs facilitate enhanced electron transfer for the redox process of $Fe(CN)_6^{3-}$/$Fe(CN)_6^{4-}$ [15, 42–44], thus increasing the effective surface area available for signal transduction. Deposition of TEOS/GOx and TMOS/GOx layers reduced electrode surface area by approximately 33 ± 6% and 10 ± 2%, while deposition of BSA/GA/GOx layer reduced surface area by an average of 15 ± 6%. Composite design schemes utilizing sol–gel layers (CNT–TEOS/CNT–TMOS) reduced the surface area by an average of 29 ± 5% and 14 ± 3%, while a composite design utilizing a covalent linking scheme (CNT–GA) reduced the surface area by an average of 28 ± 10%. For all composite designs, the effective surface area determined by the Randles–Sevcik method was decreased compared with Pt/MWNT/Nafion electrodes, due to a reduction in conductive area by sol–gel and/or BSA–GA.

3.2. Comparison of different schemes

In the absence of CNTs, biosensor sensitivity was highly dependent on the immobilization scheme (i.e., entrapment in sol–gel versus covalent linking; figures 2(a) and (b)). Biosensors utilizing TEOS exhibited the largest sensitivity (1172.2 ± 256.9 nA mM^{-1}), followed by BSA/GA/GOx biosensors (620.1 ± 56.0 nA mM^{-1}), and TMOS/GOx biosensors (395.7 ± 41.6 nA mM^{-1}). Sol–gel porosity is influenced by the orthosilicate precursor, degree of hydrolysis, and solution silica concentration [3]. The TEOS/TMOS solution was prepared with approximately 1 mol of TEOS/TMOS to 2.48 mol of H_2O. During the hydrolysis reaction, H_2O frees an ethanol or methanol group respectively, leaving reactive hydroxyl (–OH) groups on the silica molecule. These groups interact via polycondensation reactions to form the silica network. The most likely reason for TEOS/GOx biosensors to exhibit a higher glucose response over TMOS/GOx was that the TEOS layer had a wider range of porosities than the TMOS layer because of the slower hydrolysis and condensation reactions for TEOS due to steric hindrance by the larger ethoxy group [25], leading to a higher probability of enzyme entrapment within the TEOS matrix. This was supported by the fact that TMOS/GOx biosensors had a higher effective surface area compared with TEOS/GOx biosensors. Immobilization of GOx with GA produced a sensitivity lower than entrapment in TEOS, but higher than TMOS (all response times were less than 8 s in the 0–500 μM range).

Sensitivity was increased by an average of 181% and 41% for TMOS and BSA/GA biosensors when CNTs were incorporated in the matrix (1110.1 ± 15.4 nA mM^{-1} and 873.7 ± 105.5 nA mM^{-1}) (figures 2(c) and (d)). No significant increase in sensitivity was noted for TEOS designs including CNTs, although the porosity of the matrix did not play as significant of a role when CNTs were incorporated into the matrix (average sensitivity for CNT–TEOS biosensors was 1017.7 ± 46.6 nA mM^{-1}). Response time for sensors utilizing CNTs was less than 8 s.

Although the effective surface areas of biosensor designs varied (calculated by the Randles–Sevcik method), calculation of current density using equation (4) indicated that biosensors utilizing TEOS exhibited the largest current density (24.3 ± 3.3 μA mM^{-1} cm^{-2}) (figure 3(a)), followed by BSA/GA/GOx biosensors (10.4 ± 0.2 μA mM^{-1} cm^{-2}), and TMOS/GOx biosensors (6.2 ± 0.5 μA mM^{-1} cm^{-2}). The enhanced relative efficiency of TEOS/GOx biosensors is attributed to entrapment of enzymes within the porous TEOS sol–gel matrix.

The average current densities for CNT-based designs utilizing TEOS (19.1 ± 0.5 μA mM^{-1} cm^{-2}), TMOS (18.3 ± 0.5 μA mM^{-1} cm^{-2}) and BSA/GA (18.2 ± 4.1 μA mM^{-1} cm^{-2}) immobilization schemes were not statistically different when analyzed using ANOVA ($p < 0.05$, $\alpha = 0.05$). Although TEOS/GOx biosensors exhibited an average current density higher than CNT–TMOS biosensors, the standard error of the mean was significantly higher. The CNT–TMOS bionanocomposite resulted in more consistent biosensor performance, which is critical for research and clinical

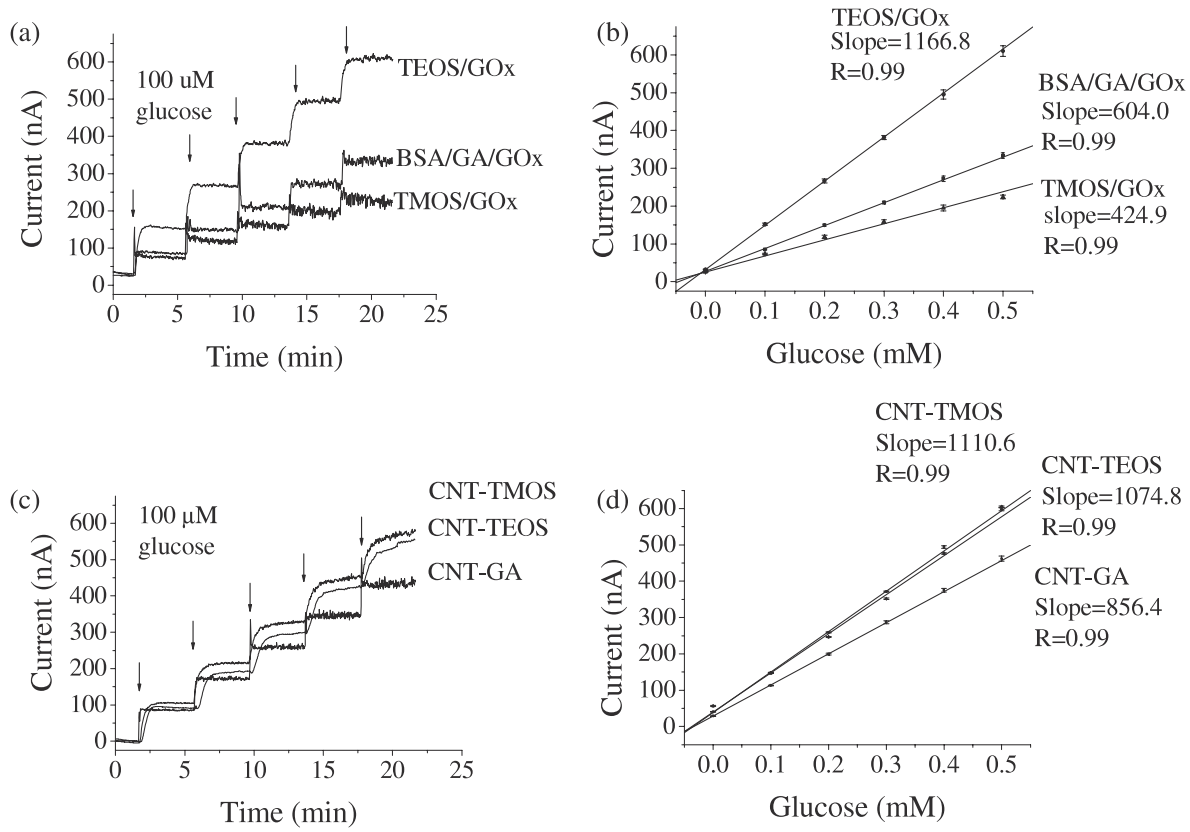

Figure 2. (a) Representative DC amperometry for glucose biosensor designs incorporating TEOS/GOx, TMOS/GOx, and BSA/GA/GOx. (b) Linear regression for average current versus glucose concentration ($n = 60$ steady state values for three replicate biosensors). (c) Representative current response to successive additions of 100 μM glucose for CNT–TMOS, CNT–TEOS and CNT–GA at a working potential of +500 mV. (d) Linear regression for average current versus glucose concentration for each CNT biosensor design. All error bars represent standard error of the arithmetic mean.

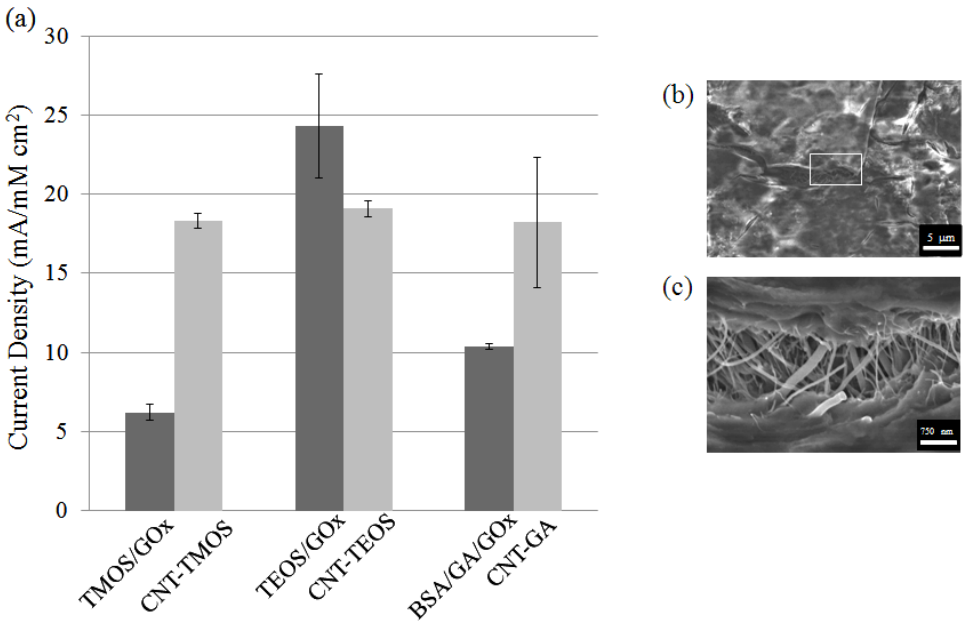

Figure 3. (a) Average current density for biosensor design schemes, (b) FESEM image of CNT–TMOS (scale bar represents 5 μm), and (c) exploded view of CNT–TMOS biosensor (scale bar represents 750 nm).

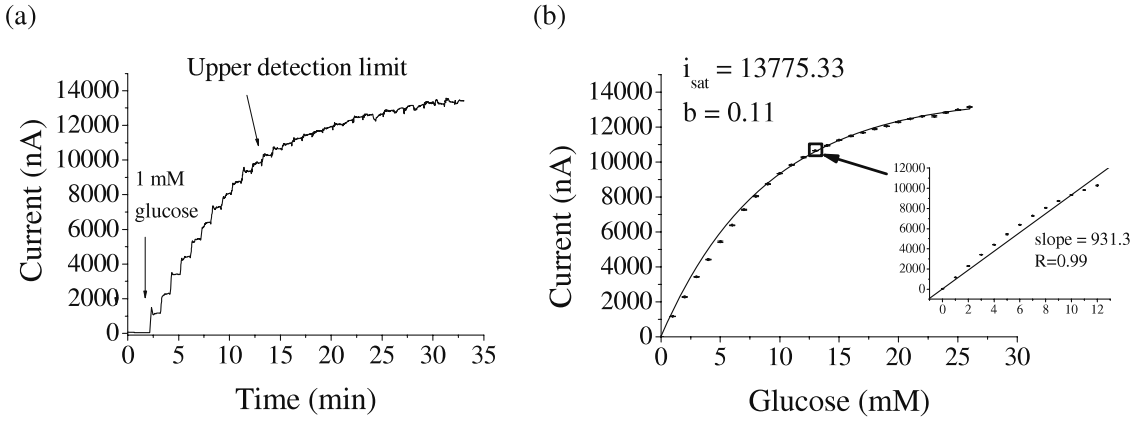

Figure 4. Representative plots demonstrating (a) the dynamic range for a CNT–TMOS biosensor, and (b) average current concentration plots for CNT–TMOS biosensor designs and exponential fits for average current versus glucose concentration up to 35 mM. The square indicates the upper detection limit (UDL). Inset: linear regression for average current versus glucose concentration up to 12 mM (UDL).

applications. For brevity, the remainder of analyses will address CNT–TMOS biosensors.

FESEM imaging indicated that the TMOS layer deposited on CNT/Nafion matrices was highly porous (figures 3(b) and (c)). The dynamic range of the CNT–TMOS biosensors was measured from 0 to 35 mM. The lower detection limit (determined using the σ_3 or 99% confidence method) was determined to be 3.7 μM, and the upper detection limit (determined using the tangential technique) was 12 mM (figure 4). This linear range covers the glucose concentration range found in human blood [7] and most cell culture media [37]. The response was exponential above 12 mM due to a combination of (i) reduced diffusive transport at the electrode surface (collapse of concentration gradient), (ii) oxygen limitations, and (iii) saturation of active enzyme binding sites. The linear range for CNT–sol–gel biosensors was significantly larger than that for CNT–GA biosensors (1.9 μM to 5 mM), demonstrating the wide range of *in vivo* and *in vitro* applications which can utilize this fabrication scheme.

Selectivity was determined by comparing response to glucose, ascorbic acid (6 μM, physiological concentration), and acetaminophen (10 μM, therapeutic concentration) for CNT–TMOS biosensors (figure 5). The current signals obtained for ascorbic acid and acetaminophen were 7.6% and 9.9% of that obtained for 1 mM glucose (typical concentration in RPMI 1640 medium for β-cell culture [37]), demonstrating desirable selectivity for glucose over common interferents typically found in blood samples. In part, the selectivity can be attributed to the negatively charged Nafion layer, which repels negatively charged molecules such as ascorbic acid and acetaminophen [29].

Although previously reported designs were successful for specific research applications, many are not well suited for a wide range of uses. This is in part due to the lack of a specific protocol for reporting biosensor performance (based on sensitivity and modified effective surface area). As demonstrated in table 1, head-to-head comparison of various designs is difficult based

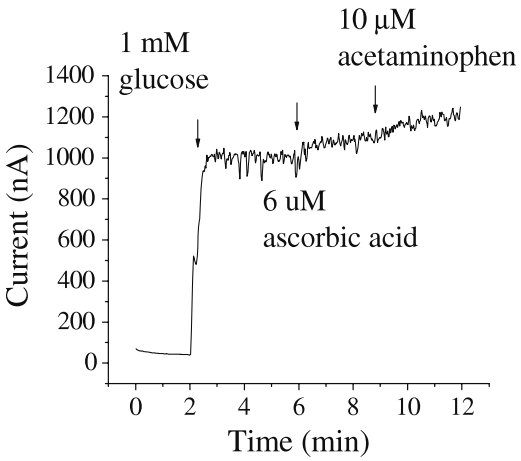

Figure 5. Selectivity test for the CNT–TMOS biosensor over 6 μM ascorbic acid and 10 μM acetaminophen in PBS. The current signals obtained for ascorbic acid and acetaminophen were 7.6% and 9.9% of those obtained for 1 mM glucose.

on sensitivity alone (even when considering electrode radius). In comparison to previous designs incorporating nanomaterials, the CNT–TMOS scheme displayed improved sensitivity, current density, detection limit and linear response range (table 1). Fabrication schemes including CNTs and sol–gel layers demonstrated improved current density over other designs in the current literature [39, 46]. Utilization of Pt improved electrochemical transduction due to the enhanced electrocatalytic capabilities [19] relative to electrodes comprised of GC [39, 47] or Au [46, 45]. GC is one of the most commonly used electrode materials [13], although the brittleness of carbon makes miniaturization difficult. Although designs by Hrapovic *et al* utilizing GC electrodes found a lower limit of detection [17], the linear sensing range did not cover expected blood glucose concentration. The stability of the CNT–TMOS design was quantified using DC potential amperometry for three consecutive days ($n = 3$ biosensors), and the results indicated no significant change in

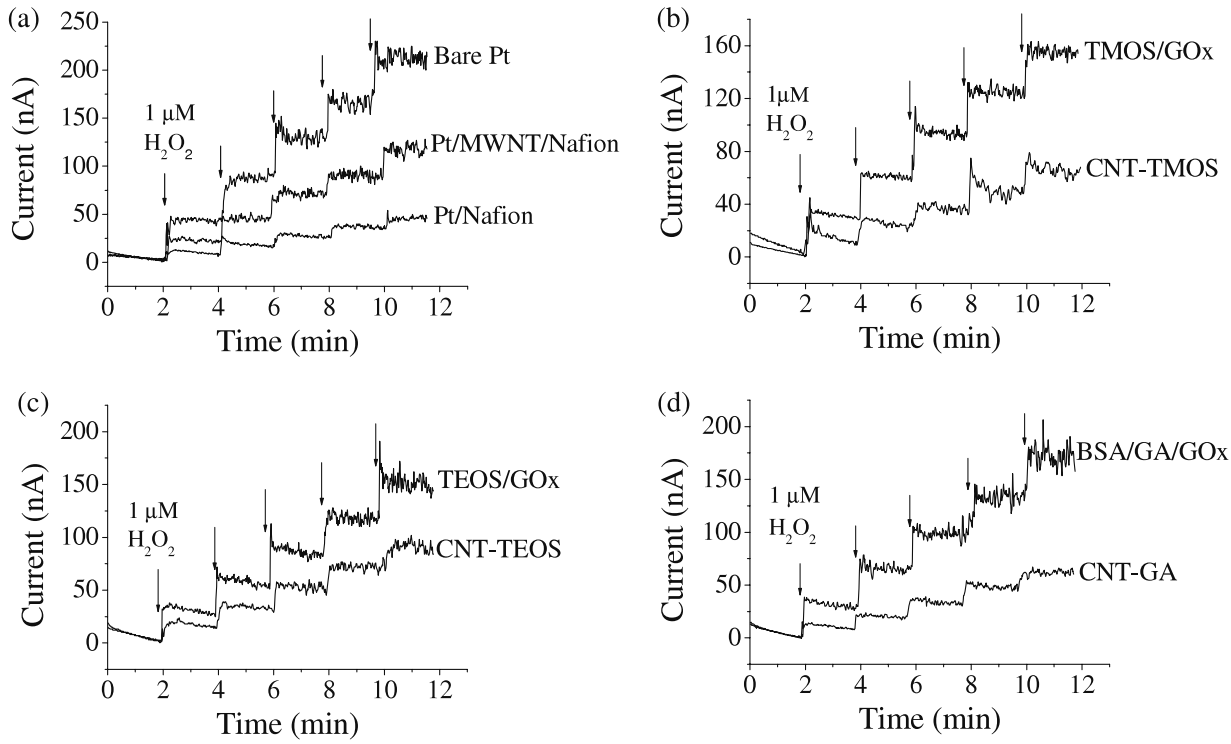

Figure 6. Representative DC amperometric response toward H_2O_2 at +500 mV for (a) a bare Pt electrode, a Pt/MWNT/Nafion electrode and a Pt/Nafion electrode, (b) a TMOS/GOx biosensor and a CNT–TMOS biosensor, (c) a TEOS/GOx biosensor and a CNT–TEOS biosensor, and (d) a BSA/GA/GOx biosensor and a CNT–GA biosensor.

Table 1. Comparison of biosensor designs incorporating various nanomaterials to fabrication schemes in the current literature. The current density was calculated based on equation (4).

Electrode description	Sensitivity (nA mM^{-1})	Electrode area (mm^2)	Sensitivity per electrode area ($\mu A\ mM^{-1}\ cm^{-2}$)	Current density ($\mu A\ mM^{-1}cm^{-2}$)	Detection limit (μM)	Linear range (mM)	Reference
CNT–TMOS	1110.1 ± 15.4	7.07	15.8 ± 0.2	18.3 ± 0.5	3.7	0.0037–12	This work
CNT–GA	873.7 ± 105.5	7.07	12.4 ± 1.5	18.2 ± 4.1	1.9	0.0019–5	This work
TEOS/GOx	1172.2 ± 256.9	7.07	16.6 ± 3.6	24.3 ± 3.3	2	0.002–8	This work
Au/cystamine/GOx	—	3.14	—	8.8 ± 0.2	8.2	0.02–5.7	[46]
Nafion/GOx/GNPs/GCE	—	7.07	—	6.5	34	up to 6	[47]
MWNT/Nafion/GOx/GCE	330	7.07	4.7	—	4	up to 2	[39]
Au/MWNT/GOx	1700	12	14.2	—	10	0.05–13	[45]
SWNT/PtNP/GCE/GOx	2110	7.07	29.7	75.4	0.5	0.0005–5	[17]

sensitivity over a three day period (average relative standard error of 2%). After 45 days of storage in 46 mg-GOx/ml-PBS at 4 °C, the sensitivity was reduced by 58%, which may be due to the loss of enzyme bioactivity during storage. This improvement in stability is significant, as previous design schemes not including sol–gel layers reported a 40% decrease in sensitivity after 50 min [38].

For all of the designs studied herein, the use of CNTs had a much larger effect on biosensor efficiency than design schemes using various combinations of (nano)materials. To explore the electrocatalytic activity of CNTs on the electrooxidation of the intermediate H_2O_2, amperometric H_2O_2 sensitivities of Pt electrodes modified with different composite layers were measured. Bare Pt electrodes had a higher average H_2O_2 sensitivity (42.0 ± 0.8 nA μM^{-1}) over Pt/Nafion electrodes (10.3 ± 2.2 nA μM^{-1}), because Nafion formed a barrier which decreased H_2O_2 diffusion [30] (figure 6(a)). Pt/MWNT/Nafion electrodes exhibited an average sensitivity (20.9 ± 0.5 nA μM^{-1}) higher than Pt/Nafion, although the sensitivity was lower than bare electrodes (figure 6(a)). This demonstrated that the MWNTs catalyzed the electrooxidation of H_2O_2, probably due to the oxygenated species on tube ends, which had been shown to increase electron transfer during H_2O_2 oxidation [8].

Glucose was measured through two steps. The first step was the conversion of glucose into H_2O_2 by GOx (biorecognition), and the second step was the electrooxidation of H_2O_2. Although the CNT–TMOS biosensors exhibited

enhanced glucose sensing performance over TMOS/GOx, biosensors modified with CNT–TMOS bionanocomposite exhibited lower H_2O_2 response (12.8 ± 1.9 nA μM^{-1}) than TMOS/GOx composite (28.6 ± 1.1 nA μM^{-1}), demonstrating that the second step of glucose sensing (electrooxidation) was not enhanced for the bionanocomposite (figure 6(b)). This was because although the MWNTs increased the electrochemical transduction, the diffusion barrier by Nafion within the bionanocomposite resulted in a H_2O_2 response lower than TMOS/GOx. Thus, the reason for the enhanced glucose sensing performance of the CNT–TMOS over the TMOS/GOx might be improved biorecognition due to an increased GOx loading or better preserved GOx activity. Since TMOS sol–gel is well known for preserving GOx activity even as well as buffer solution [18], the reason was most likely to be an increased enzyme loading in the bionanocomposite. The increased enzyme loading could be partially attributed to the unique structure of the carboxylated MWNTs used in this study, which is known for the highly porous/condensed matrices, entrapping enzymes via electrostatic/hydrophobic interactions and peptide bonds [13, 45]. Similar results on H_2O_2 response were observed with other bionanocomposites, where CNT–TEOS (18.0 ± 1.4 nA μM^{-1}) had lower H_2O_2 response than TEOS/GOx (23.1 ± 5.6 nA μM^{-1}) (figure 6(c)), and CNT–GA had lower H_2O_2 response (13.7 ± 2.6 nA μM^{-1}) than BSA/GA/GOx (28.7 ± 6.0 nA μM^{-1}) (figure 6(d)).

Several available biosensor fabrication schemes incorporating nanomaterials were demonstrated in this work, and novel biosensors could be developed based on the demonstrated designs. With the different designs, there were multiple variables (e.g., enzyme concentration) that would result in different biosensing performances. The optimization of each design, such as using different types of CNTs (e.g., aligned single-walled carbon nanotubes) and the inclusion of other nanomaterials (e.g., metal nanoparticle) could further improve the biosensing performance [28, 37]. The proposed protocol based on current density enabled the comparison of different schemes, and also enabled the study of the impacts of variables which were inherent in each scheme by evaluating the integrative effect of these variables on biosensing. This would lead to future improved biosensor designs. In this study, a uniform GOx concentration and dip coating were used for the enzyme immobilization of each design, which further standardized the comparative analysis.

4. Conclusions

In this study, glucose biosensors based on various nanomaterial construction approaches (TEOS/GOx, TMOS/GOx, BSA/GA/GOx, CNT–TMOS, CNT–TEOS and CNT–GA) were studied and compared based on both sensitivity and nanomaterial-modified surface area (i.e., current density). Performance comparison protocols considering current density are vital for accurate head-to-head comparison of biosensor design schemes. Using this protocol, CNT–TMOS immobilized on a Pt electrode was the optimum design in terms of enhanced current density (18.3 ± 0.5 $\mu A\ mM^{-1}\ cm^{-2}$), linear range (0.0037–12 mM), low detection limit (3.7 μM), coefficient of variation in sensitivity (2%), response time (less than 8 s), and reproducibility relative to other glucose biosensor designs in the recent literature. The results from H_2O_2 response tests showed that the enhanced performance was most likely due to an increased enzyme loading in the CNT–TMOS bionanocomposite. The use of the anion repellent Nafion layer repelled common electrochemical interferents typically found in blood samples and resulted in desirable selectivity. This bionanocomposite CNT–TMOS biosensor is well suited for clinical and other practical biosensor applications. The linear sensing range is indicative of the wide range of *in vivo* and *in vitro* applications which can utilize this fabrication scheme. Comparison of designs based on rational combinations of nanomaterials using a consistent protocol possesses great engineering significance for optimization of biosensor fabrication in both academic and industrial settings.

Appendix

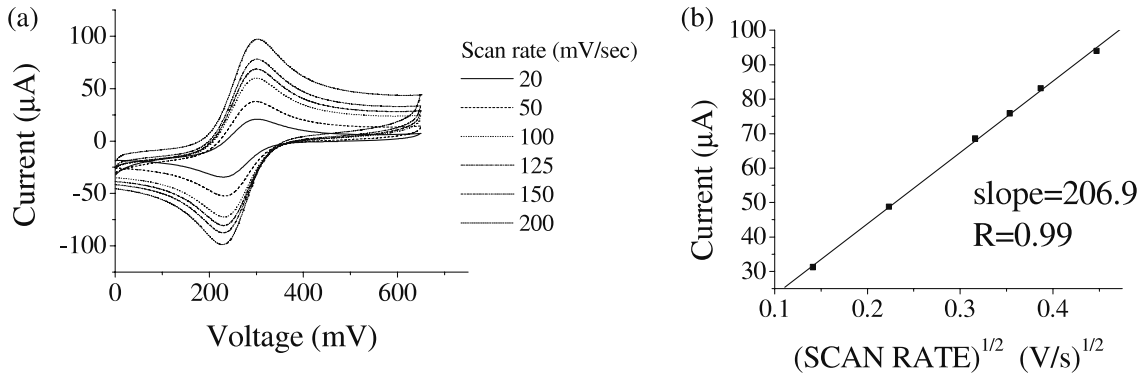

Figure A.1. (a) Representative cyclic voltammogram in ferricyanide for a bare Pt electrode at various scan rates (mV s^{-1}). (b) Linear regression between the peak current (i_p) and the square root of the scan rate ($v^{1/2}$) for a 1.5 mm radius bare platinum electrode. The average surface area determined using the Randles–Sevcik equation was 7.07 ± 0.16 mm^2, and the average radius was 1.50 ± 0.02 mm.

References

[1] Badea M, Curulli A and Palleschi G 2003 Oxidase enzyme immobilisation through electropolymerised films to assemble biosensors for batch and flow injection analysis *Biosens. Bioelectron.* **18** 5–6

[2] Bard A J and Faulkner L R 2000 *Electrochemical Methods: Fundamentals and Applications* (New York: Wiley)

[3] Brinker C J and Scherer G W 1990 *Sol–gel Sci.* p 97

[4] Burmeister J J, Pomerleau F, Palmer M, Day B K, Huettl P and Gerhardt G A 2002 Improved ceramic-based multisite microelectrode for rapid measurements of-glutamate in the CNS *J. Neurosci. Methods* **119** 163–71

[5] Busk M, Horsman M R, Kristjansen P E G, van der Kogel A J, Bussink J and Overgaard J 2008 Aerobic glycolysis in cancers: implications for the usability of oxygen-responsive genes and fluorodeoxyglucose-PET as markers of tissue hypoxia *Int. J. Cancer* **122** 2726–34

[6] Chen H and Dong S 2007 Direct electrochemistry and electrocatalysis of horseradish peroxidase immobilized in sol–gel-derived ceramic-carbon nanotube nanocomposite film *Biosens. Bioelectron.* **22** 1811–5

[7] Choleau C, Klein J C, Reach G, Aussedat B, Demaria-Pesce V, Wilson G S, Gifford R and Ward W K 2002 Calibration of a subcutaneous amperometric glucose sensor implanted for seven days in diabetic patients: part 2. Superiority of the one-point calibration method *Biosens. Bioelectron.* **17** 647–54

[8] Chou A, Bocking T, Singh N K and Gooding J J 2005 Demonstration of the importance of oxygenated species at the ends of carbon nanotubes for their favourable electrochemical properties *Chem. Commun.* 842–4

[9] Claussen J C, Franklin A D, ul Haque A, Porterfield D M and Fisher T S 2009 Electrochemical biosensor of nanocube-augmented carbon nanotube networks *ACS Nano* **3** 37–44

[10] Claussen J C, Kim S S, Haque A U, Artiles M S, Porterfield D M and Fisher T S 2010 Electrochemical glucose biosensor of platinum nanospheres connected by carbon nanotubes *J. Diabetes. Sci. Technol.* **4** 312–9

[11] Day B K, Pomerleau F, Burmeister J J, Huettl P and Gerhardt G A 2006 Microelectrode array studies of basal and potassium-evoked release of l-glutamate in the anesthetized rat brain *J. Neurochem.* **96** 1626–35

[12] Garcia E J, Wardle B L, John Hart A and Yamamoto N 2008 Fabrication and multifunctional properties of a hybrid laminate with aligned carbon nanotubes grown *in Situ Compos. Sci. Technol.* **68** 2034–41

[13] Gong K, Yan Y, Zhang M, Su L, Xiong S and Mao L 2005 Electrochemistry and electroanalytical applications of carbon nanotubes: a review *Anal. Sci.* **21** 1383–94

[14] Gong K, Zhang M, Yan Y, Su L, Mao L, Xiong S and Chen Y 2004 Sol–gel-derived ceramic-carbon nanotube nanocomposite electrodes: tunable electrode dimension and potential electrochemical applications *Anal. Chem.* **76** 6500–5

[15] Gooding J J 2005 Nanostructuring electrodes with carbon nanotubes: a review on electrochemistry and applications for sensing *Electrochim. Acta* **50** 3049–60

[16] Guerrieri A, De Benedetto G E, Palmisano F and Zambonin P G 1998 Electrosynthesized non-conducting polymers as permselective membranes in amperometric enzyme electrodes: a glucose biosensor based on a co-crosslinked glucose oxidase/overoxidized polypyrrole bilayer *Biosens. Bioelectron.* **13** 103–12

[17] Hrapovic S, Liu Y, Male K B and Luong J H 2004 Electrochemical biosensing platforms using platinum nanoparticles and carbon nanotubes *Anal. Chem.* **76** 1083–8

[18] Kunzelmann U and Bottcher H 1997 Biosensor properties of glucose oxidase immobilized within SiO_2 gels *Sensors Actuators* B **39** 222–8

[19] Li X, Heryadi D and Gewirth A A 2005 Electroreduction activity of hydrogen peroxide on Pt and Au electrodes *Langmuir* **21** 9251–9

[20] Liaw H W, Chen J M and Tsai Y C 2006 Development of an amperometric ethanol biosensor based on a multiwalled carbon nanotube–Nafion–alcohol dehydrogenase nanobiocomposite *J. Nanosci. Nanotechnol.* **6** 2396–402

[21] Lin Y, Lu F, Tu Y and Ren Z 2004 Glucose biosensors based on carbon nanotube nanoelectrode ensembles *Nano Lett.* **4** 191–5

[22] Llaudet E, Hatz S, Droniou M and Dale N 2005 Microelectrode biosensor for real-time measurement of ATP in biological tissue *Anal. Chem.* **77** 3267–73

[23] Lowry J P, O'Neill R D, Boutelle M G and Fillenz M 1998 Continuous monitoring of extracellular glucose concentrations in the striatum of freely moving rats with an implanted glucose biosensor *J. Neurochem.* **70** 391–6

[24] Makino K, Maruo S, Morita Y and Takeuchi T 1988 A study on the glutaraldehyde activation of hydrophilic gels for immobilized enzymes *Biotechnol. Bioeng.* **31** 617–9

[25] McDonagh C, Bowe P, Mongey K and MacCraith B D 2002 Characterisation of porosity and sensor response times of sol–gel-derived thin films for oxygen sensor applications *J. Non-Cryst. Solids* **306** 138–48

[26] McLamore E S, Diggs A, Calvo Marzal P, Shi J, Blakeslee J J, Peer W A, Murphy A S and Porterfield D M 2010 Non-invasive quantification of endogenous root auxin transport using an integrated flux microsensor technique *Plant J.* **63** 1004–16

[27] McLamore E S, Mohanty S, Shi J, Claussen J, Jedlicka S S, Rickus J L and Porterfield D M 2010 A self-referencing glutamate biosensor for measuring real time neuronal glutamate flux *J. Neurosci. Methods* **189** 14–22

[28] McLamore E S *et al* 2011 A self referencing platinum nanoparticle decorated enzyme-based microbiosensor for real time measurement of physiological glucose transport *Biosens. Bioelectron.* **26** 2237–45

[29] Ni J, Ju H, Chen H-Y and Leech D 1999 Amperometric determination of epinephrine with an osmium complex and Nafion double-layer membrane modified electrode *Anal. Chim. Acta* **378** 151–7

[30] Pan S and Arnold M A 1996 Selectivity enhancement for glutamate with a Nafion/glutamate oxidase biosensor *Talanta* **43** 1157–62

[31] Qi W, Yan X, Duan L, Cui Y, Yang Y and Li J 2009 Glucose-sensitive microcapsules from glutaraldehyde cross-linked hemoglobin and glucose oxidase *Biomacromolecules* **10** 1212–6

[32] Rickus J L, Dunn B and Zink J I 2002 *Optical Biosensors: Present and Future* ed F S Ligler and C A Rowe Taitt (Amsterdam: Elsevier Science) pp 427–56

[33] Salimi A, Compton R G and Hallaj R 2004 Glucose biosensor prepared by glucose oxidase encapsulated sol–gel and carbon-nanotube-modified basal plane pyrolytic graphite electrode *Anal. Biochem.* **333** 49–56

[34] Schalkhammer T, Mann-Buxbaum E, Pittner F and Urban G 1991 Electrochemical glucose sensor on permselective non-conducting substituted pyrrole polymers *Sensors Actuators* B **4** 273–81

[35] Schuhmann W 1991 Amperometric substrate determination in flow-injection systems with polypyrrole-enzyme electrodes *Sensors Actuators* B **4** 41–9

[36] Shi J, Cha T, Claussen J, Diggs A, Choi J H and Porterfield D M 2011 Microbiosensors based on DNA modified single-walled carbon nanotube and Pt black nanocomposites *Analyst* at press

[37] Shi J, McLamore E, Jaroch D, Claussen J, Rickus J and Porterfield D M 2011 Oscillatory glucose flux in INS1 pancreatic [beta] cells: a self-referencing microbiosensor study *Anal. Biochem.* **411** 185–93
[38] Tsai Y-C and Chiu C-C 2007 Amperometric biosensors based on multiwalled carbon nanotube–Nafion–tyrosinase nanobiocomposites for the determination of phenolic compounds *Sensors Actuators* B **125** 10–6
[39] Tsai Y C, Li S C and Chen J M 2005 Cast thin film biosensor design based on a Nafion backbone, a multiwalled carbon nanotube conduit, and a glucose oxidase function *Langmuir* **21** 3653–8
[40] Van Benschoten J J 1983 Cyclic voltammetry experiment *J. Chem. Educ.* **60** 772–6
[41] Wang G X, Ahn J H, Yao J, Lindsay M, Liu H K and Dou S X 2003 Preparation and characterization of carbon nanotubes for energy storage *J. Power Sources* **119/121** 16–23
[42] Wang J 1999 Amperometric biosensors for clinical and therapeutic drug monitoring: a review *J. Pharm. Biomed. Anal.* **19** 1–2
[43] Wang J 2005 Carbon-nanotube based electrochemical biosensors: a review *Electroanalysis* **17** 7–14
[44] Wang J, Musameh M and Lin Y 2003 Solubilization of carbon nanotubes by Nafion toward the preparation of amperometric biosensors *J. Am. Chem. Soc.* **125** 2408–9
[45] Wang S G, Zhang Q, Wang R, Yoon S F, Ahn J, Yang D J, Tian J Z, Li J Q and Zhou Q 2003 Multi-walled carbon nanotubes for the immobilization of enzyme in glucose biosensors *Electrochem. Commun.* **5** 800–3
[46] Zhang S, Wang N, Yu H, Niu Y and Sun C 2005 Covalent attachment of glucose oxidase to an Au electrode modified with gold nanoparticles for use as glucose biosensor *Bioelectrochemistry* **67** 15–22
[47] Zhao S, Zhang K, Bai Y, Yang W and Sun C 2006 Glucose oxidase/colloidal gold nanoparticles immobilized in Nafion film on glassy carbon electrode: direct electron transfer and electrocatalysis *Bioelectrochemistry* **69** 158–63
[48] Zou Y, Xiang C, Sun L-X and Xu F 2008 Glucose biosensor based on electrodeposition of platinum nanoparticles onto carbon nanotubes and immobilizing enzyme with chitosan–SiO_2 sol–gel *Biosens. Bioelectron.* **23** 1010–6